Environ Fluid Mech (2016) 16:87–100
DOI 10.1007/s10652-015-9414-3

ORIGINAL ARTICLE

Rapid operation of a Tainter gate: generation process and initial upstream surge motion

Simin Sun[1] · Xinqian Leng[1] · Hubert Chanson[1]

Received: 23 January 2015 / Accepted: 20 April 2015 / Published online: 29 April 2015

Abstract In water supply channels, the brusque operation of control gates may induce large unsteady flow motion called surges. Such a rapid operation of gates must often be restricted, although it may be conducted to scour silted channels and sewers. Herein a physical study was conducted under controlled flow conditions to study the turbulent mixing in the very-close vicinity of a rapidly opening/closing Tainter gate, with a focus on the unsteady transient mixing induced by the gate operation. The data suggested that the negative/positive surge generation was associated with large instantaneous free-surface fluctuations. The velocity measurements indicated significant variations in longitudinal velocity during the surge generation, as well as large fluctuations of all velocity components. The processes were associated with large Reynolds stress levels. A succession of rapid closure and opening of undershoot gates provided optimum conditions to scour silted canals, and the present results gave some detailed insights into the physical processes.

Keywords Hydraulic transients · Open channels · Tainter gate · Physical modelling · Rapid operation · Surge generation · Unsteady turbulence · Free-surface motion · Physical modelling · Desilting

1 Introduction

In rivers and canals, regulation structures are commonly installed to control the open channel flow motion. One type of regulation device is the underflow gate for which there is an extensive literature dealing with the operation in steady flow conditions [1–4]. In water supply channels, the brusque operation of control gates may induce large unsteady flow

✉ Hubert Chanson
h.chanson@uq.edu.au;
http://www.uq.edu.au/~e2hchans/

1 School of Civil Engineering, The University of Queensland, Brisbane, QLD 4072, Australia

motion called surges (Fig. 1) which might overtop the channel banks, damaging and eroding the channel. In practice, a rapid operation of gates must often be restricted, although it might be unavoidable in emergency situations.

Positive and negative surges may be analysed using the Saint-Venant equations and the method of characteristics in channels of simple shapes [5–7]. These analytical solutions were recently tested against some limited laboratory study [8, 9]. The results showed that the surge generation process was very poorly modelled by the Saint-Venant equations. This was linked to the inadequacy of the Saint-Venant equations. The one-dimensional equations cannot provide a precise description of two- and three-dimensional unsteady flows [7, 10], including during surge generation. Altogether, there is limited information on the transient hydraulics of undershoot gate operation, despite some extensive literature on open channel transients [11, 12]. The impact of rapid unsteady gate motion was rarely investigated in the close vicinity of the gate, except in the context of sediment removal [13, 14] and weir calibration [15]. The present contribution aims to address this knowledge gap.

It is the purpose of this contribution to study thoroughly the surge generation process and unsteady flow motion in the very-near upstream proximity of a Tainter gate during both fast opening and closure. New measurements were conducted in a relatively large size facility ($S_0 = 0$, L = 12 m, W = 0.5 m). The results gave a new perspective into negative and positive surge generation, and associated transient turbulent processes, as well as a

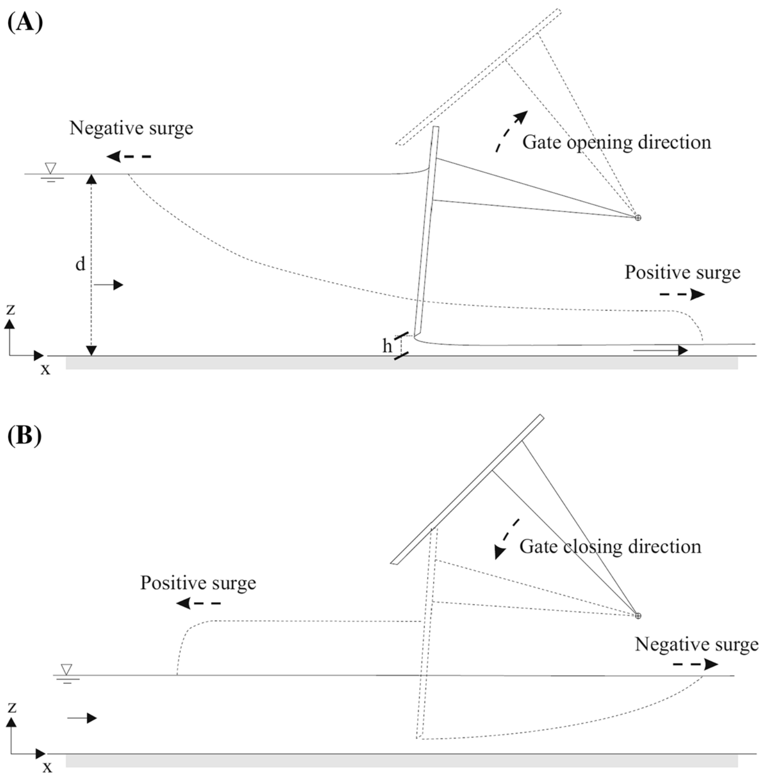

Fig. 1 Sketch of hydraulic transients generated by undershoot gate operation in a canal: **a** rapid gate opening and **b** rapid gate closure

systematic comparison between the distinctively different surges. The study provided a detailed data set for future computational fluid dynamics studies of gate opening and closure.

2 Experimental investigations

2.1 Facility and instrumentation

New experiments were conducted in a 12 m long 0.5 m wide channel at the University of Queensland. The bed was made out of PVC and the glass sidewalls were 0.3 m high. The bed slope was horizontal. The waters were supplied by a constant head tank and the 12 m long glass sidewall channel was fed by an intake structure equipped with flow straighteners and meshes followed by a smooth sidewall and bottom convergent. A Tainter gate made of smooth marine ply was located next to the channel's downstream end ($x_{Gate} = 11.12$ m) where x is the distance from the test section's upstream end (Fig. 2). Thus the gate's inflow conditions were fully-developed as documented during preliminary measurements. The Tainter gate was 0.53 m high and a dimensioned sketch is presented in Fig. 2 (Right). The horizontal channel ended with a free-overfall located 0.88 m downstream of the gate.

The water discharge was measured with an orifice meter calibrated on site with a percentage of error less than 2 %. In steady flows, the water depth was measured using rail mounted pointer gauges. The unsteady flow depth was recorded non-intrusively with a series of acoustic displacement meters (ADMs) Microsonic™ Mic + 25/IU/TC. A sensor was located at x = 11.25 m immediately downstream of the Tainter gate. Three acoustic displacement meters were placed upstream of and close to the gate at x = 10.9, 10.3, and 9.7 m, while two sensors were placed further upstream at x = 8 m and x = 5 m. The acoustic displacement meters were calibrated against the pointer gauges in steady flows. In addition, the free-surface profiles were documented with some video movies collected with a digital camera Samsung™ Galaxy Note II N7100 (30 fps, 1280 p × 800 p), and complemented by digital photographs taken with a Pentax™ K-7 dSLR camera. The movies

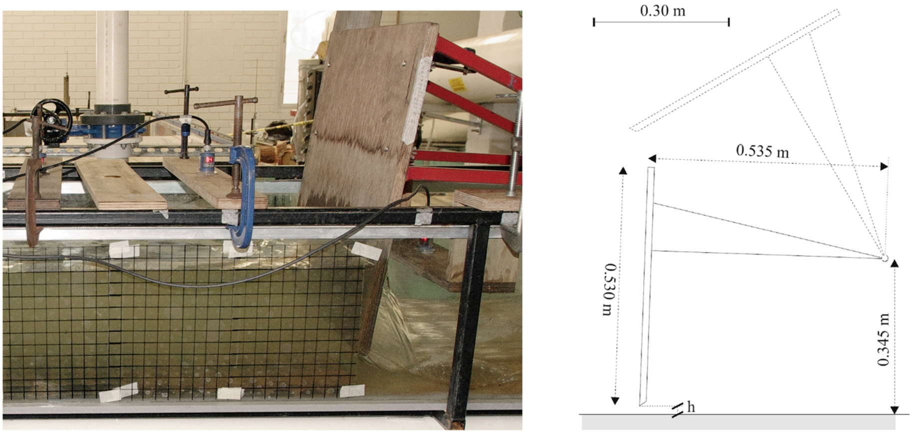

Fig. 2 Partially-closed Tainter gate with flow direction from *left to right*—photograph (*Left*) for Q = 0.0354 m^3/s and h = 85 mm, and dimensioned sketch (*Right*)

and photographs were taken through the right sidewall. The free-surface tracking was performed using a frame by frame analysis and the video image processing was manual to guarantee maximum reliability of the data.

The velocity measurements were conducted using an acoustic Doppler velocimeter (ADV) Nortek™ Vectrino+ (Serial No. VNO 0436) equipped with a three-dimensional side-looking head located at $x = 10.9$ m. The velocity range was 1.0 m/s and the sampling rate was 200 Hz. The ADV was set up with a transmit length of 0.3 mm and a sampling volume of 6 mm diameter and 1.5 mm height. Both the acoustic displacement meters and ADV were synchronised within ±1 ms, and sampled simultaneously at 200 Hz.

The error on the pointer gauge data was 0.5 mm. The accuracy of the acoustic displacement meter data was ±0.2 mm [16]. The error on the water elevation deduced from photographic and video observations was less than 1 mm. The velocity data accuracy was 1 % of the velocity range i.e., ±1 cm/s [17].

2.2 Experimental flow conditions

The present experiments were selected with the same initially steady discharge to investigate the transient flow motion induced by a rapid gate operation (Table 1). The experimental flow conditions are summarised in Table 1, where Q is the initially steady flow discharge, d is the water depth and h is the undershoot gate opening.

The same experimental protocol was applied to each experimental run. The steady gradually-varied flow conditions were established for at least 5 min prior to the gate motion. The surge was generated by the rapid operation of the Tainter gate and its propagation was studied immediately upstream of the gate. A rapid opening induced an upstream negative surge while a rapid closure generated a positive surge propagating upstream (Fig. 1). The gate opening/closure time was between 0.1 and 0.2 s, and such a

Table 1 Experimental investigations of rapid Tainter gate opening and closure

Run	Tainter gate motion	Initial flow conditions				Surge generation	Instrumentation
		Q (m^3/s)	h	d_0/d_c	Re		
A	Rapid gate opening (complete opening)	0.0345	0.066	2.60	1.5×10^5	Negative surge propagating upstream	Acoustic displacement meters (25 runs), acoustic
B1	Rapid gate closure (partial closure: $h = 0.068$ m)	0.0345	N/A	1.31	1.9×10^5	Undular positive surge propagating upstream	Doppler velocimetry (25 runs), & video-camera (25 runs)
B2	Rapid gate closure (complete closure: $h = 0$)	0.0345	N/A	1.31	1.9×10^5	Breaking positive surge propagating upstream	

d water depth, d_c critical flow depth $d_c = (q^2/g)^{1/3}$, d_0 initial water depth measured at $(x_{Gate} - x) = 6.12$ m, *h* undershoot gate opening, *Q* initially steady flow discharge, *Re* Reynolds number defined in terms of the hydraulic diameter, *x* longitudinal distance from the upstream end of the glass sidewall test section, x_{Gate} tainter gate location $x_{Gate} = 11.12$ m

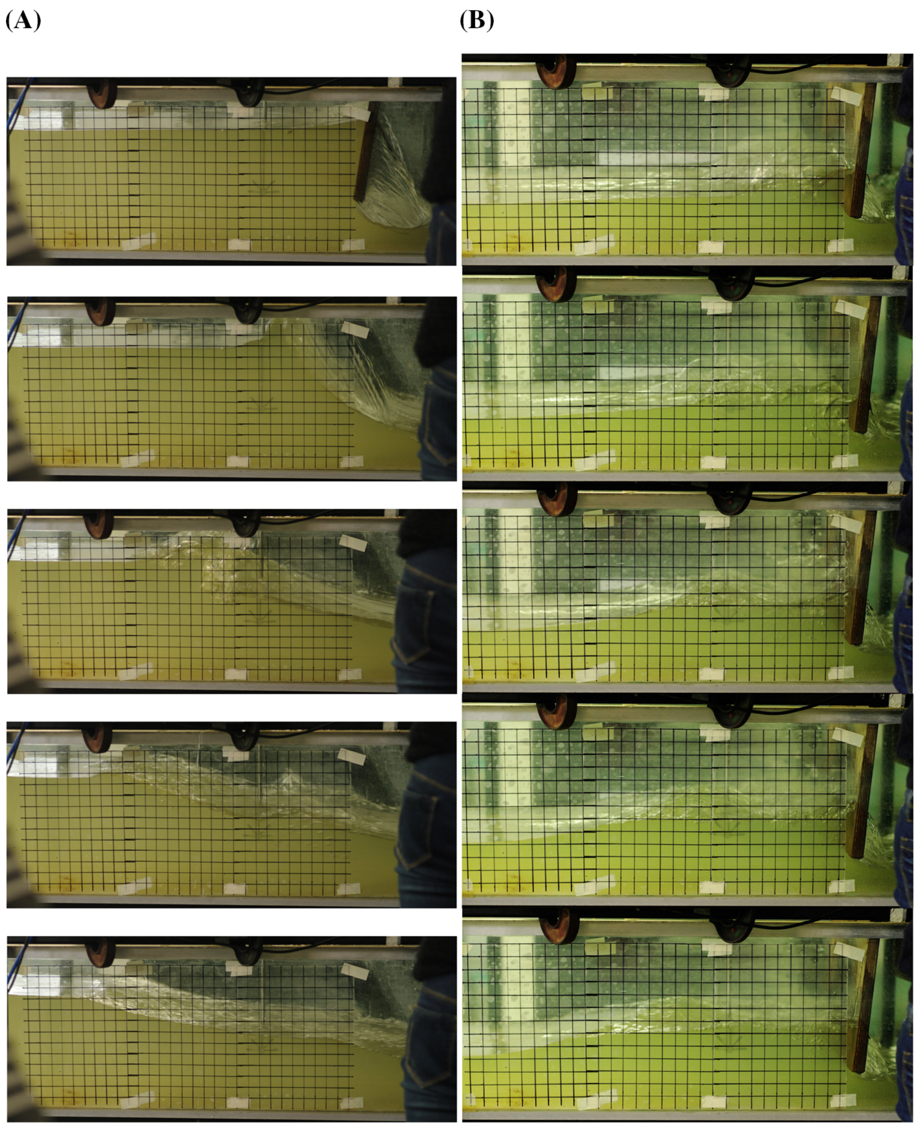

Fig. 3 Rapid gate opening/closure sequences viewed through the right sidewall with initial flow direction from *left to right*—from *top to bottom*, 0.19 s between photographs. (A, *Left*) Rapid gate opening sequence (run A, Q = 0.0345 m^3/s, h = 66 mm). (B, *Right*) Rapid gate closure sequence (run B1, Q = 0.0345 m^3/s, h = 56 mm)

short opening/closure time had little effect on the surge propagation. After opening/closure, the measurements stopped when the surge leading edge reached the upstream end of the glass wall channel to prevent any reflection effect. Each experimental run was repeated carefully 25 times and all the data (ADMs, video, ADV) were ensemble-averaged following the approach of [18].

3 Basic observations

3.1 Flow patterns

The rapid gate operation generated surges propagating both upstream and downstream of the gate, although the main focus of this study was the upstream surge propagation. During the rapid opening experiment (run A, Table 1), a negative surge propagated upstream. A small disturbance was observed next to and immediately upstream of the gate corresponding to the upward motion of a small volume of displaced fluid. The displaced fluid fell back into the flow and the initial disturbance vanished rapidly as the fluid was advected in the downstream direction. This is seen in Fig. 3a presenting a sequence of photographs taken during the gate opening, with 0.19 s between two successive photographs. The negative surge propagated further upstream, the instantaneous free-surface profile exhibiting a very-smooth shape. All visual observations indicated the gradual lowering of the water surface, upstream of the gate, during the upstream propagation of the surge, and the surge leading edge was barely perceptible, as previously reported [19, 20]. The rapid gate opening was also associated with the formation of a positive surge downstream of the gate,

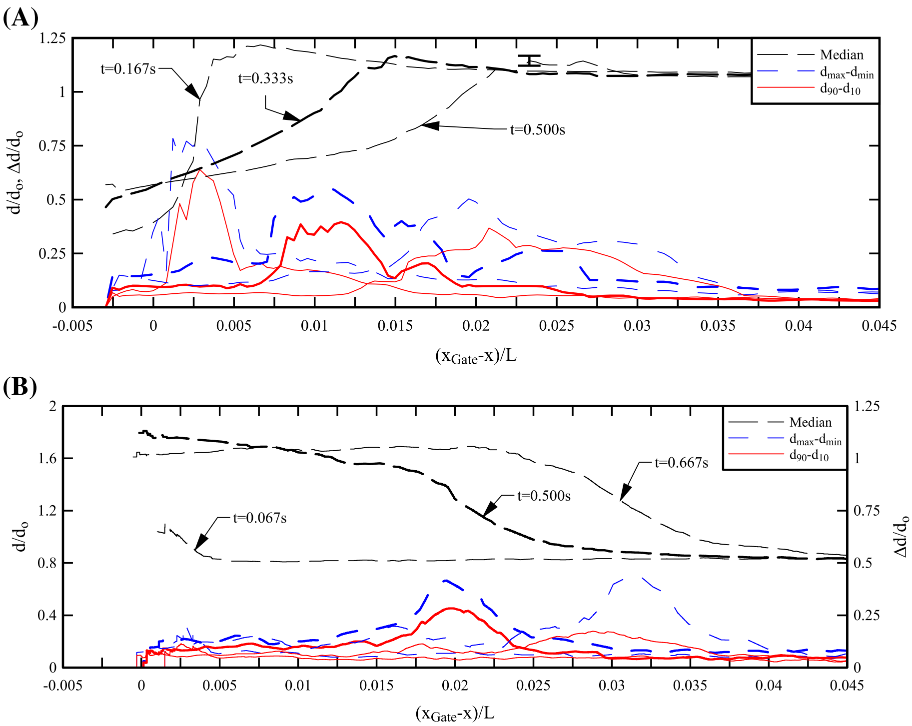

Fig. 4 Instantaneous free-surface profiles immediately upstream of the gate after rapid gate operation—Video-camera data (25 runs), upstream surge propagation from *left to right*. **a** Ensemble-averaged median free-surface profile and free-surface fluctuations during a negative surge generation (Run A)—From top to bottom: 0.167, 0.333 and 0.50 s after gate opening. **b** Ensemble-averaged median free-surface profile and free-surface fluctuations during a positive surge generation (Run B2)—From *top to bottom*: 0.067, 0.50 and 0.667 s after gate closure

although its free-surface characteristics were only recorded at x = 11.25 m (i.e. $x_{Gate} - x = -0.13$ m). The positive surge front reached very rapidly the free-overfall.

The fast closure of the gate (Runs B1 & B2, Table 1) induced a positive surge propagating upstream. Run B1 corresponded to to a partial gate closure which generated an undular positive surge further upstream. Run B2 was a complete gate clsoure inducing the generation of a bore with a marked breaking roller. In both cases, the rapid closure induced some water pile-up against the gate and the formation of a turbulent roller, before the roller detached from the gate and propagated upstream. This is seen in Fig. 3b. A comparison between Fig. 3a, b shows further some key differences between the generation of negative and positive surges. The positive surge generation was highly turbulent, as previously reported by [8, 21]. Its upstream propagation induced a major flow disturbance in the upstream channel. Altogether the generation of the positive surge was a slower process

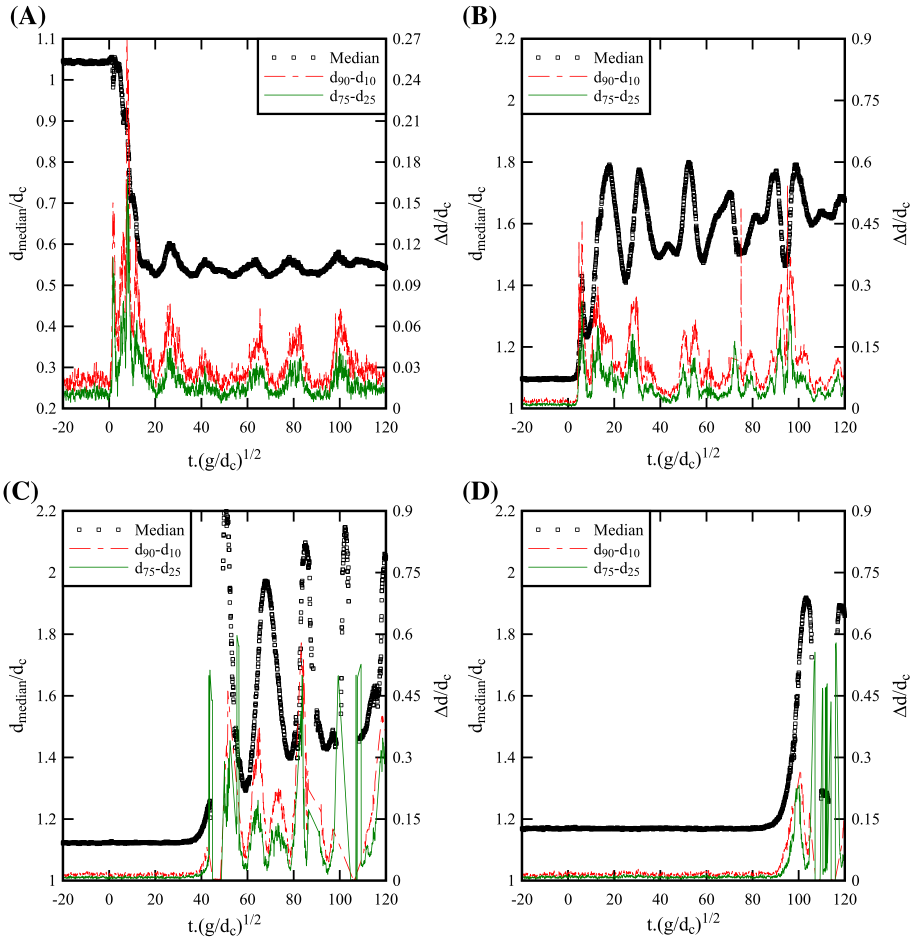

Fig. 5 Time-variation of ensemble-averaged median water depth and free-surface fluctuations during rapid gate closure (Run B1)—Acoustic displacement meter data (25 runs), centreline data. **a** Downstream of gate: $x_{Gate} - x = -0.13$ m **b** Upstream of gate: $x_{Gate} - x = +0.22$ m. **c** Upstream of gate: $x_{Gate} - x = +0.82$ m **d** Upstream of gate: $x_{Gate} - x = +3.12$ m

than the formation of the negative surge, and its upstream propagation was slower than that of a negative surge, as predicted by basic theoretical considerations [5, 7]. The fast gate closure was also associated with a negative surge propagating downstream of the gate.

3.2 Free-surface measurements

The video ensemble-average data were analysed in terms of the instantaneous median water surface, the difference between ninth and first deciles ($d_{90}-d_{10}$) of the data ensemble, and the difference between maximum and minimum values ($d_{max}-d_{min}$). For a Gaussian distribution of the ensemble around its mean ($d_{90}-d_{10}$) would be equal to 2.6 times the standard deviation [22]. Both ($d_{90}-d_{10}$) and ($d_{max}-d_{min}$) provided some quantitative measure of the instantaneous free-surface fluctuations. Typical data are presented in Fig. 4a, b, where t is the time since gate opening and closure respectively, d_o is the initial flow depth (Table 1), L is the channel length (L = 12 m) and the gate location was $x = x_{Gate}$ (i.e. $x_{Gate} - x = 0$). During the generation of both negative and positive surges, the experimental data showed a maximum in free-surface fluctuations $(d_{90}-d_{10})_{max}$ occurring slightly after the surge leading edge (Fig. 4). Interestingly the negative surge generation produced comparatively and quantitatively larger free-surface fluctuations than the positive surge generation for the same initial discharge: e.g., at t = 0.50 s, $(d_{90}-d_{10})_{max}$ was larger during the negative surge generation (Fig. 4). The finding may appear counter-intuitive since the negative surge appeared to be a more gentle process than the positive surge further upstream. It might reflect however some key differences in terms of turbulent mixing during the surge generation.

The video data were complemented by free-surface elevation measurements using the acoustic displacement meters. The ensemble-averaged data showed the same qualitative and quantitative results as the video data, highlighting that the surge generation was a quasi-two-dimensional process in terms of the free-surface profile. Typical data are presented in Fig. 5 for a rapid gate closure, in terms of the instantaneous median water depth, the difference between ninth and first deciles ($d_{90}-d_{10}$) of the data ensemble, and the difference between third and first quartiles ($d_{75}-d_{25}$), where d_c is the critical flow depth ($d_c = \sqrt[3]{q^2/g}$), q is the initial discharge per unit width, and g is the gravity acceleration. Figure 5 shows both the negative surge generated downstream of the gate (Fig. 5a) and the upstream propagation of an undular positive upstream of the gate (Fig. 5b–d). Note a few data spikes and missing data points in Fig. 5c, d reflecting the limitations of the sensors when the acoustic beams were not reflected back to the sensor: e.g. in presence of sloping water surface. Overall the data shown in Fig. 5 illustrate the generation and upstream propagation of an undular positive surge.

4 Velocity measurements

During the surge generation (Table 1), the instantaneous velocity components V_x, V_y and V_z were sampled simultaneously on the channel centreline 0.35 m upstream of the gate, i.e. $(x_{Gate} - x)/d_c = 2.8$, with V_x the longitudinal velocity component positive downstream, V_y the transverse velocity positive towards the left sidewall and V_z the vertical velocity positive upwards. The instantaneous velocity recordings were repeated 25 times and the data were ensemble-averaged. The data ensemble were analysed in terms of the instantaneous median and instantaneous velocity fluctuation ($V_{90}-V_{10}$) that is the difference between the 9th and 1st deciles. Typical results are presented in Figs. 6 and 7, where V_c is the critical flow velocity ($V_c = \sqrt[3]{g \times q}$). Note in Fig. 6 that each median velocity curve V/V_c is offset vertically by +0.2 from the lower data set.

For the generation of an upstream negative surge (Run A), the data showed the rapid flow acceleration at all elevations during the rundown of the water surface (Fig. 6 Top). The flow acceleration was linked with an increase in instantaneous fluctuations for all velocity components. The velocity fluctuations were consistently larger than during the initially steady flow. There was however some difference between velocity components in terms of fluctuating quantities. The longitudinal velocity measurements showed very large velocity fluctuations during the initial stage of the surge generation as illustrated in Fig. 6 (Top) for $2.5 < t \times (g/d_c)^{1/2} < 15$. The other velocity components showed large fluctuations without this distinctive peak. The transverse velocity V_y was zero on average in the initially steady flow, and the surge generation induced some fluctuations in V_y about zero. On the other hand, the drawdown of the water surface was associated with some negative vertical velocities, particularly close to the free-surface (Fig. 6 Bottom). Indeed,

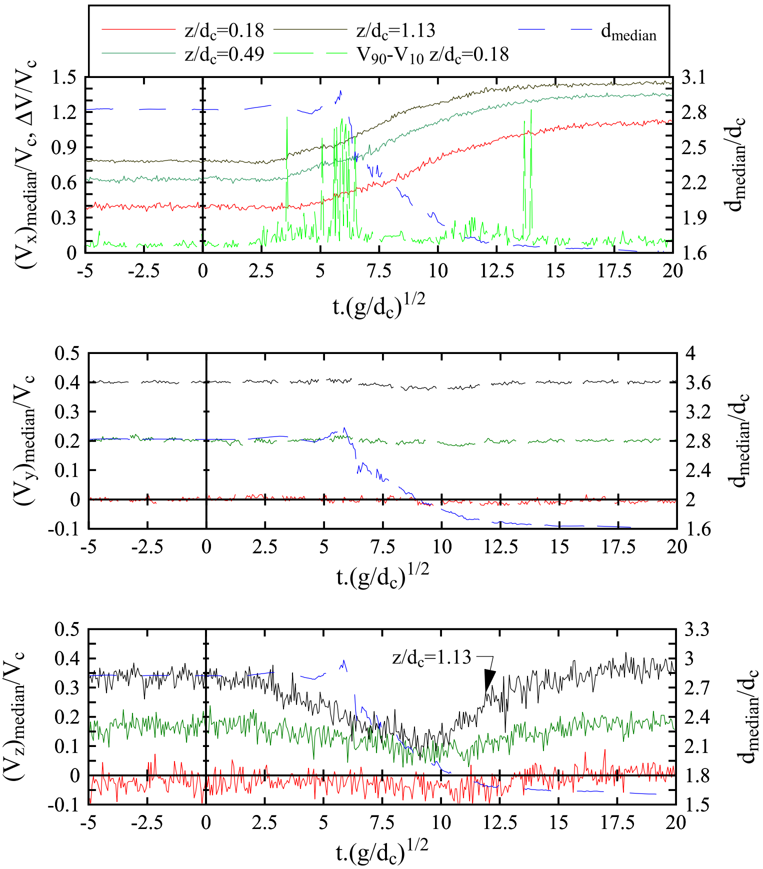

Fig. 6 Ensemble-average median free-surface profile, median velocity components and velocity fluctuations at 0.35 m upstream of the gate ($x_{Gate} - x = 0.35$ m) during a negative surge generation (Run A)—Each median velocity curve V/V_o is offset vertically by +0.2 from the previous one

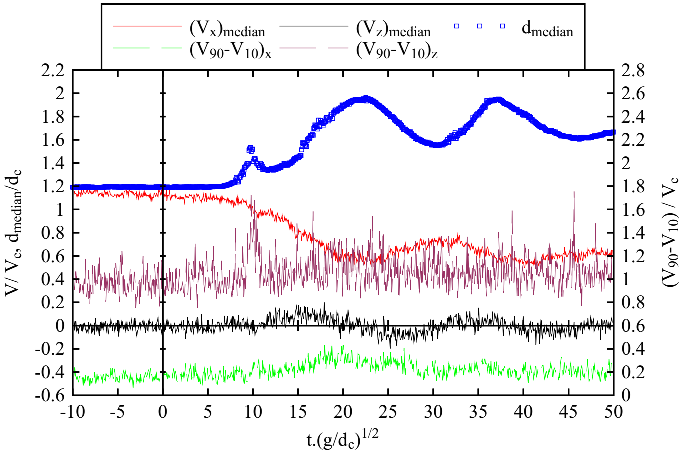

Fig. 7 Ensemble-average median free-surface profile, median velocity components and velocity fluctuations at z = 0.0388 m ($z/d_c = 0.49$) and 0.35 m upstream of the gate ($x_{Gate} - x = 0.35$ m) during a positive surge generation (Run B1)

at the free-surface, the vertical velocity component must satisfy the no-flow-through condition:

$$V_z(z = d) = (\partial z/\partial t)_{z=d} \quad (1)$$

where d is the water depth and z is the vertical elevation above the bed. Overall it was believed that the increase in velocity fluctuations observed during and after negative surge propagation indicated some intense turbulent mixing at all vertical elevations. The present findings were consistent with the earlier observations of [19].

With the generation of positive surges, the velocity measurements showed that the surge generation and upstream propagation induced a rapid flow deceleration (Fig. 7). This is illustrated in Fig. 7. During the generation of the breaking surge (Run B2), some large fluctuations of longitudinal, transverse and vertical velocity components were observed beneath the surge. The maximum horizontal and vertical velocity fluctuations occurred about the same time as the maximum free-surface fluctuations (see above). The transverse velocity data presented some large fluctuations after the surge front, implying some intense secondary motion in the wake of the surge. In the undular surge (Run B1), the surge leading edge was followed with a train of secondary waves (Figs. 5, 7), which affected all three velocity components. This is illustrated in Fig. 7 in which the horizontal velocity component V_x was minimum beneath the wave crests and oscillated with the same period as the free-surface undulations but out of phase. The vertical and transverse velocity presented a similar oscillating pattern beneath the free-surface undulations. Note that the longitudinal velocity deceleration was more gentle than during the generation of the breaking surge.

5 Discussion

Large instantaneous fluctuations in velocity were recorded upstream of the gate during the generations of the surges. The maximum instantaneous fluctuations were comparable for the positive and negative surges. Indeed the generation processes were highly turbulent.

Further the data showed large instantaneous turbulent Reynolds stresses during the surge generation (Fig. 8). Figure 8 presents the time variations of the first and ninth deciles of the tangential stress $\rho \times v_x \times v_z$, the ninth decile of the normal stress $\rho \times v_x^2$ and the water depth. The results showed comparatively larger instantaneous turbulent stress magnitudes during the generation of a positive surge, although the generation of both positive and negative surges induced large stress levels. Maximum shear stresses were observed typically beneath the leading edge of the negative/positive surges, with maximum median shear stresses up to 20–50 Pa and maximum instantaneous shear stress in excess of 120 Pa.

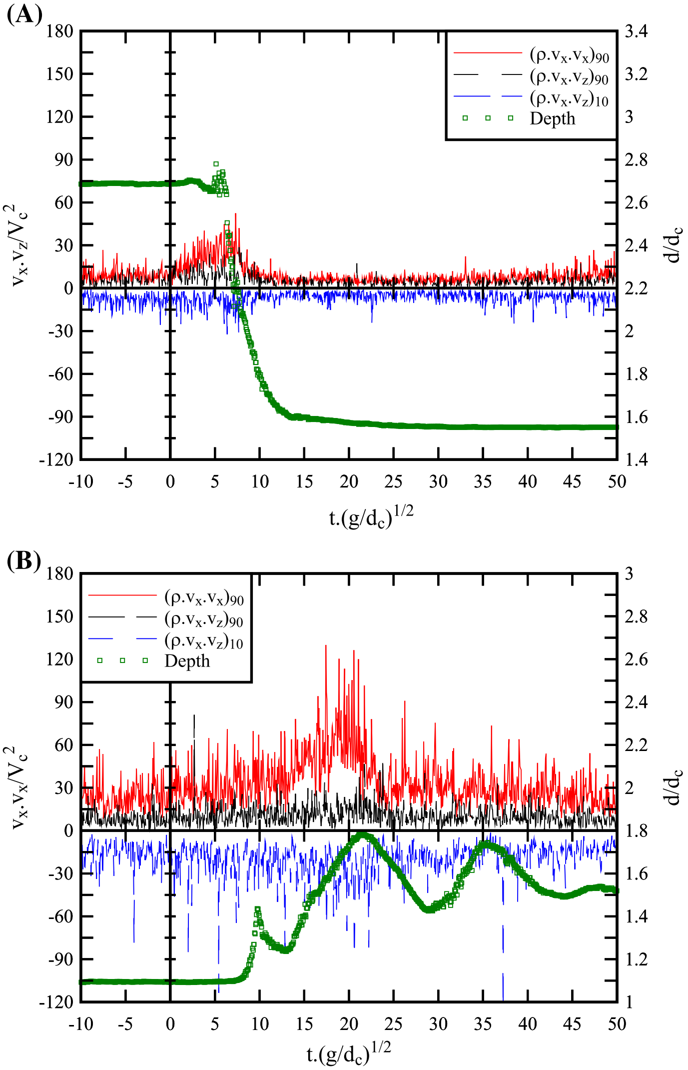

Fig. 8 Time variation of water depth, ensemble's ninth decile of normal stress $\rho \times v_x \times v_x$ and first and ninth deciles of tangential stress $\rho \times v_x \times v_z$ during the surge motion upstream of the gate—Flow conditions: $Q = 0.0345$ m^3/s, $x = 10.9$ m (i.e. $x_{Gate} - x = 0.35$ m), $z/d_c = 0.17$. **a** Negative surge generation (Run A). **b** Positive surge generation (Run B1)

For comparison, the Shields diagram predicts a critical shear stress for sediment motion of 0.1–0.5 Pa for fine sand particles [23]. In natural systems, recent field observations yielded critical shear stress data for cohesive sediment erosion between 0.1 and 10 Pa [24, 25]. Herein the measured instantaneous stress levels were one to two orders of magnitude larger than the critical threshold for sediment motion of both fine cohesive and non-cohesive materials. The results indicated that the surge generation can scour a mobile bed located upstream of the gate, during both negative and positive surge transient. In a practical application, a rapid gate closure followed by a rapid gate opening may provide the optimum conditions to scour intensely the sediment bed upstream of the gate which will be advected downstream during the acceleration phase following the rapid gate opening (Fig. 9). The process might be applied to remove sediments in silted canals and a similar technique is already used in sewers with a movable fast tilting floodgate [13]. The sediment removal is a dual-action process, taking place upstream and downstream of the gate with the successive generation of positive and negative surges downstream, and negative and positive surges upstream (Fig. 9). This is sketched in Fig. 9. Practically, the opening and

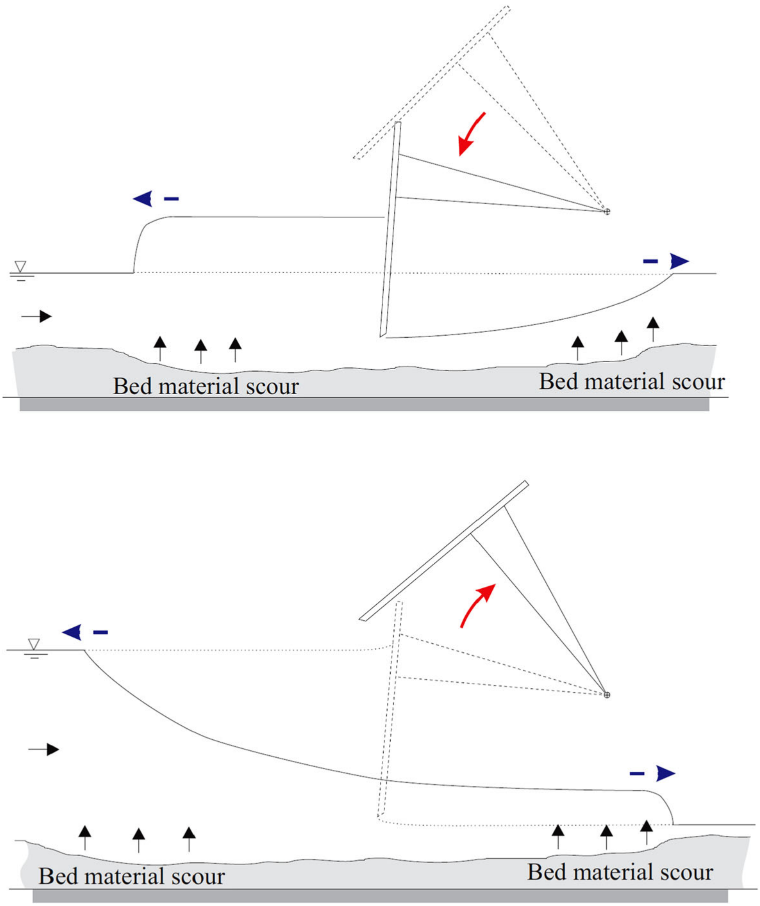

Fig. 9 Sketch of bed scour and sediment removal during successive rapid gate closure (*Top*) and opening (*Bottom*) in a heavily silted channel

closure manoeuvres must be repeated, while the feasibility, effectiveness and safety of such operations will need to be tested with mobile bed experiments.

6 Conclusion

The generation of positive and negative surges by rapid gate closure and opening was investigated experimentally in a relatively large size facility with a range of complementary instrumentation. The focus of the study was a fine characterisation of the instantaneous free-surface elevations and velocity fluctuations in the very close upstream proximity of the Tainter gate during the rapid gate operation. The free-surface and velocity measurements were repeated 25 times and the results were ensemble-averaged. The free-surface measurements (video and acoustic displacement sensor) highlighted the rapid deformation of the free-surface immediately upstream of the gate during the positive/negative surge generation process. The ensemble-averaged data suggested that the surge generation was a quasi-two-dimensional flow, albeit large instantaneous free-surface fluctuations were observed at the surge leading edge. The instantaneous velocity measurements indicated significant variations in longitudinal velocity during the positive/negative surge generation, as well as large fluctuations in all velocity components. The large instantaneous velocity fluctuations were associated with large Reynolds stress magnitudes.

The successive rapid closure and opening of the gate provide the optimum conditions to scour silted channels, with the scour materials being rapidly advected downstream after the gate operation. A similar method is already implemented in sewers. The present results gave some detailed insights into the physical processes, highlighting a dual-action scour process taking place both downstream and upstream of the rapidly moving gate. The present data set could further be used to validate the numerical modelling of positive/negative surge generation, as indeed the numerical approach is challenging because of the intense turbulence generated during the gate operation, as well as the large and rapid free surface deformations.

Acknowledgments The authors thank the reviewers for the helpful comments. They acknowledge the technical assistance of Jason Van Der Gevel and Matthew Stewart, School of Civil Engineering at the University of Queensland. The financial support of the Australian Research Council (Grant DP120100481) is acknowledged.

References

1. Metzler DE (1948) A model study of Tainter-gate operation. M.Sc. Thesis, University of Iowa, Dept of Mechanics and Hydraulics, August, 22 pages
2. Lewin J (1985) Hydraulic gates and valves in free surface flow and submerged outlets. Thomas Telford, London, p 238
3. Henderson FM (1966) Open channel flow. MacMillan Company, New York
4. Montes JS (1997) Irrotational flow and real fluid effects under planar sluice gates. J Hydrau Eng, ASCE 123(3):219–232
5. Liggett JA (1994) Fluid mechanics. McGraw-Hill, New York
6. Sturm TW (2001) Open channel hydraulics., Water resources and environmental engineering seriesMcGraw Hill, Boston, p 493
7. Chanson H (2004) Environmental hydraulics of open channel flows. Elsevier-Butterworth-Heinemann, Oxford, p 483

8. Reichstetter M (2011) Hydraulic modelling of unsteady open channel flow: physical and analytical validation of numerical models of positive and negative surges. MPhil thesis, School of Civil Engineering, The University of Queensland, Brisbane, p 112
9. Simon B, Chanson H (2013) Turbulence measurements in tidal bore-like positive surges over a rough bed. *Hydraulic* Model Report No. CH90/12, School of Civil Engineering, The University of Queensland, Brisbane, p 176
10. Montes JS (1998) Hydraulics of open channel flow. ASCE Press, New-York, p 697
11. Cunge J, Holly FM, Verwey A (1980) Practical aspects of computational river hydraulics. Boston, Pitman, p 420
12. Chaudhry MH (2008) Open channel flow, 2nd edn. Springer, New York
13. Riochet B (2008) La Sédimentation dans les Réseaux Unitaires Visitables: le Point de Vue d'un Exploitant. ('Sedimentation in Large Combined Sewage Systems: Perspectives of an Operator.') In: Bouguenais, Larrarte F, Chanson H (eds) Proceedings international meeting on measurements and hydraulics of sewers IMMHS'08, Summer School GEMCEA/LCPC, 19–21 Aug. 2008, Hydraulic Model Report No. CH70/08, Univ. of Queensland, Brisbane, pp 11–19 (in French)
14. Williams KJ, Tait SJ, Ashley RM (2009) In-sewer sedimentation associated with active flow control. Water Sci Technol 60(1):55–63
15. Chanson H, Wang H (2013) Unsteady discharge calibration of a large V-notch weir. Flow Meas Instrum 29:19–24. doi:10.1016/j.flowmeasinst.2012.10.010
16. Microsonic (2009) Instruction manual: mic + ultrasonic sensors with one analogue output. Microsonic GmbH, Dortmund, p 3
17. Nortek (2009) Vectrino velocimeter user guide. Nortek AS, Norway, p 42
18. Chanson H, Docherty NJ (2012) Turbulent velocity measurements in open channel bores. Eur J Mech B/Fluids 32:52–58. doi:10.1016/j.euromechflu.2011.10.001
19. Reichstetter M, Chanson H (2013) Negative surges in open channels: physical and numerical modeling. J Hydraul Eng ASCE 139(3):341–346. doi:10.1061/(ASCE)HY.1943-7900.0000674
20. Leng X, Chanson H (2015) Negative surges and unsteady turbulent mixing induced by rapid gate opening in a channel. Exp Therm Fluid Sci 63:133–143. doi:10.1016/j.expthermflusci.2014.06.015
21. Lubin P, Chanson H, Glockner S (2010) Large eddy simulation of turbulence generated by a weak breaking tidal bore. Environ Fluid Mech 10(5):587–602. doi:10.1007/s10652-009-9165-0
22. Spiegel MR (1972) Theory and problems of statistics. McGraw-Hill Inc., New York
23. Graf WH (1971) Hydraulics of sediment transport. McGraw-Hill, New York
24. Sanchez M, Levacher D (2008) Erosion d'une vase de l'estuaire de la Loire sous l'action du courant (Erosion of a mud from the Loire estuary by a flow). Bull Eng Geol Environ 67:597–605. doi:10.1007/s10064-008-0159-9
25. Jacobs W, Le Hir P, Van Kesteren W, Cann P (2011) Erosion threshold of sand–mud mixtures. Cont Shelf Res 31(10):S14–S25. doi:10.1016/j.csr.2010.05.012